Self-Assembly, *In Vitro* Gene Transfection, and Antimicrobial Activity of Biodegradable Cationic Bolaamphiphiles

Pabitra Mondal, Joykrishna Dey,* Sadhana Roy, and Somdeb Bose Dasgupta

Read Online

ACCESS | Metrics & More | Article Recommendations | Supporting Information

ABSTRACT: Bolaamphiphiles or bolaforms have drawn particular interest in drug and gene delivery, and studies of bolaforms have been growing continuously. Bolaforms, due to their unique structure, exhibit specific self-assembly behavior in water. The present work aims to develop biodegradable cationic bolaforms with a better gene transfection ability. In this work, a novel cationic bolaform (Bola-1) with head groups bearing hydroxyl (OH) functionality was designed and synthesized to investigate self-assembly and gene transfection efficiency. The self-assembly behavior of Bola-1 in water was compared with that of the hydrochloride salt (Bola-2) of its precursor molecule to investigate the effect of the −OH functionality on their solution properties. Several techniques, including surface tension, electrical conductivity, fluorescence probe, calorimetry, dynamic light scattering, and atomic force microscopy, were employed for the physicochemical characterization of Bola-1 and Bola-2. Despite the presence of polar urea groups in the spacer chain, both bolaforms were found to form spherical or elongated micelles above a relatively low critical aggregation concentration (CAC). The presence of the OH group was found to significantly affect the CAC value. The results of calorimetric measurements suggested a thermodynamically favorable aggregate formation in salt-free water. Despite stronger binding efficiency with calf thymus DNA, *in vitro* gene transfection studies performed using adherent cell Hek 293 suggested that both Bola-1 and Bola-2 have gene transfection efficiency comparable to that of turbofectamine standard. Both bolaforms were found to exhibit significant *in vitro* cytotoxicity at higher concentrations. Also, the bolaforms showed beneficial antibacterial activity at higher concentrations.
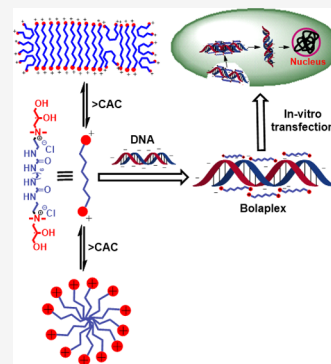
INTRODUCTION

Bolaamphiphiles have received massive attention due to their unique structure, which makes them exhibit some special functions different from those of conventional single-headed amphiphiles. Bolaamphiphiles, also called bolaforms, are characterized by two polar head groups linked through a hydrophobic spacer with one or two alkyl chains.[1] The hydrophilic groups on a bolaform can be ionic or nonionic and identical or different. Different head groups can provide additional properties to the amphiphile, thus allowing for precise control of the property of the amphiphile. The noncovalent interactions between bolaform molecules in water can form various nanostructures such as vesicles, lamellae, disks, spherical and rod-like micelles, tubules, ribbons, and fibers of sizes in a micro- and nanometer range.[2] In fact, bolaforms, in comparison to single-headed amphiphiles, are found to be more appropriate building blocks for the fabrication of functional supramolecular architectures in the laboratory.[1,3−10] These properties also allow them to find practical applications in sensor technology, microreactors, imaging, and catalytic reactions.[11−16] Over the past few decades, studies to establish the relationship between the microstructure of self-assembled aggregates and chemical structures have led to the development of novel synthetic bolaforms. The results obtained from studies on these synthetic bolaform molecules have suggested the existence of

complex relationships between chain composition, spacers, and head groups that considerably influence the microstructure of their self-assembled aggregates.[17−24] It has been observed that a long spacer (C18 or higher) between the two polar head groups leads to the formation of micelles and a short spacer (C12−C18) leads to vesicle formation. The nature of counterions has also been found to influence the aggregation behavior of bolaforms.[2,25] It is well known that the monolayer lipid membranes (MLMs) of bolaform vesicles are more tightly packed and less permeable in comparison to bilayer membranes of liposomes.[26] The monolayer arrangement of the membrane provides the vesicle with higher stability, encapsulation efficiency, and an efficiently controlled release mechanism.[1] These advantages make bolaform vesicles (bolasomes) attractive candidates for the delivery of small molecular drugs, proteins, and nucleic acids. Researchers have effectively encapsulated water-soluble fluorescent

markers,[20−22] peptides,[23] and DNA[27,28] and delivered them across biological barriers.

The aggregation behavior of cationic bolaforms in the presence of DNA provides context for special applications, such as DNA purification and transfection to a cell's nucleus. Cationic bolaforms have been employed in various applications, including gene delivery. It has been reported that bolasomes prepared from cationic bolaforms in the presence of lipids such as 1,2-dioleyl-*sn*-glycero-3-phosphoethanolamine are capable of delivering genes to target cells.[29] Following the report by Eaton and co-workers[30] on using cationic bolaforms as a nonviral gene delivery vector, several cell- and mitochondria-targeting cationic bolaforms have been developed.[31−35] Although the transfection efficiency of these bolaforms was observed to be not satisfactory, the cationic surfaces have been shown to promote transcytosis enhancing vesicle transport across biological barriers,[36] mainly through the blood−brain barrier (BBB).[37,38] The potential advantages of cationic bolaforms as building blocks of vesicles for drug delivery led researchers to study their self-assembly properties.[20−24] However, the relationships between different chemical structures and applications, such as gene transfection, need to be fully understood. For example, the role of quaternary ammonium head groups containing hydrophilic groups, such as hydroxyls (−OH), on the self-assembly behavior, DNA binding, and gene transfection efficiency is yet to be investigated. Past studies on several cationic single-chain and gemini surfactants with quaternary ammonium head groups containing one or more hydroxyethyl moieties have shown greater transfection efficiency.[39−42] It has also been suggested that incorporating two or more hydroxyalkyl moieties in the headgroup reduces toxicity.[41,42] On the other hand, another group of researchers reported that increased covalent distances between the hydroxyl functionality and the cationic centers of glycolipids with hydroxyalkyl head groups adversely affected transfection efficiencies.[43,44]

This study aims to develop cationic bolaforms with low toxicity and better gene transfection efficiency. Accordingly, in this work, we designed and synthesized a cationic bolaform (Bola-1; Figure 1a) with two symmetrical quaternary
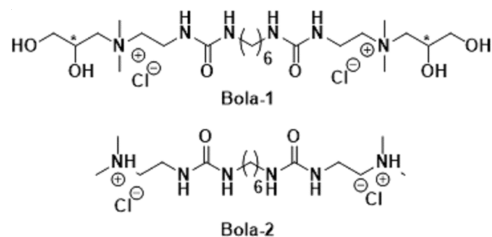

Figure 1. Molecular structures of (a) Bola-1 and (b) Bola-2.

ammonium head groups, each bearing a dihydroxypropyl moiety. The cationic head groups are connected to the two ends of a six-carbon (C_6) alkyl chain through urea linkages. The incorporation of bis-ureido groups in the molecule gives rise to strong intermolecular hydrogen-bonding interactions, which have been utilized to produce organogels[45] and hydrogels.[46] In recent years, urea-containing compounds have received much attention due to their growing application in drug design and medicinal chemistry.[47] The urea functionality is incorporated into the structure of drug molecules to modulate drug potency and selectivity and

improve drug properties.[48] The urea linkages may also have beneficial effects on self-assembly formation. Also, the urea linkage is not spontaneously hydrolyzed in solution and, hence, is very stable. Thus, the present study is undertaken to investigate the effects of urea linkages and −OH groups in the quaternary ammonium head on the aggregation behavior and gene transfection ability of Bola-1 as well as of the dihydrochloride salt (Bola-2; Figure 1b) of its precursor containing tertiary amine groups. Further, the effects of −OH moieties on DNA binding, *in vitro* DNA transfection efficiency and cytotoxicity, and antibacterial effects have been investigated.

■ EXPERIMENTAL SECTION

Materials. *N,N*-Dimethylethylenediamine (98%), 3-chloro-1,2-dihydroxypropane (98%), 1,6-diisocyanatohexane (97%), *N*-phenyl-1-naphthylamine (NPN, 98%), 1,6-diphenyl-1,3,5-hexatriene (DPH), ethidium bromide (EB), 3-(4,5-dimethylthiazolyl-2)-2,5 diphenyltetrazolium bromide (MTT), and D_2O (99.6 atom % D) were obtained from Sigma-Aldrich (Bangalore, India). Ethidium bromide (EB), ct-DNA (sodium salt, ex. calf thymus (highly polymerized)), glycerol (99.5%), and sodium chloride (99.9%) were purchased from SRL (Mumbai, India). The fluorescent probes NPN and DPH were recrystallized from an acetone−ethanol (50:50 v/v) mixture two times before use. The similarity of the fluorescence excitation spectrum with the absorption spectrum of the probes confirmed its purity. HEK 293 cell lines were obtained from NCCS Pune. GFP VIVIT DNA was obtained from Addgene. Dulbecco's modified Eagle's medium-high glucose was purchased from Sigma-Aldrich. Turbofect transfection reagent was obtained from Thermo Fischer Scientific. *Staphylococcus aureus* and *Escherichia coli* were obtained from IMTech, (Chandigarh). Isopropyl alcohol, dichloromethane (DCM), MeOH and triethylamine (TEA, 98%), and sulfuric acid (98%) were purchased from Merck (Mumbai, India). Methanol, isopropyl alcohol, DCM, and TEA were further dried and distilled before use. Milli-Q water (18 MΩ·cm; pH = 6.7) was used to prepare aqueous solutions.

Synthesis of Bolaforms. The bolaforms were synthesized according to the standard procedure reported in the literature.[49,50] Details are available in the Supporting Information (SI). The chemical structures of Bola-1 and Bola-2 were identified by FT-IR, ^{1}H, ^{13}C NMR, and HRMS spectroscopy. The chemical identification data and representative FT-IR, ^{1}H, ^{13}C NMR, and HRMS spectra (Figures S1−S7) are included in the SI.

General Instrumentation. FT-IR spectra were recorded on a PerkinElmer (model spectrum RX 1) spectrometer using a KBr pellet. All ^{1}H and ^{13}C NMR spectra were recorded on a Bruker (400 and 500 MHz) NMR spectrometer using MeOH-d_4/D_2O as the chemical shift reference for mode-locking. The melting points of compounds were measured with an INSTIND melting point system (Kolkata, India).

Surface Tension Measurements. Surface tension (γ) measurements were carried out with a surface tensiometer (Jencon (India), Kolkata-28, SL. NO-353) using the Du Nüoy ring method. The instrument was calibrated by measuring the surface tension of Milli-Q water. The γ value was measured by successive addition of aliquots of different bolaform stock solutions to 25 mL of Milli-Q water in a glass beaker. The solution was gently stirred for 2 min and then equilibrated for another 5 min at 25 °C before γ was measured. Each measurement was repeated three times to minimize any error.

Conductivity Measurements. A Thermo-Orion digital conductivity meter (model 150 A+) that uses a conductivity cell with a cell constant of 0.467 cm^{-1} was used for conductivity measurements. The instrument was calibrated by measuring the conductivity of a standard salt solution. The κ value was measured after successive addition of aliquots of bolaform stock solution to 25 mL of Milli-Q water taken in a water-jacketed beaker placed on a magnetic stirrer. The solution was gently stirred for 1 min and equilibrated for 5 min to get a constant κ value. Each measurement was repeated three times to

minimize any error. A JULABO MC circulating water bath with a temperature accuracy of ±0.1 K was used to control the temperature of the solution.

Steady-State and Time-Resolved Fluorescence Measurements. The steady-state fluorescence spectra of NPN and EB probes were recorded on a Shimadzu RF-6000 series instrument that uses LabSolutions RF (version 1.11) software. For fluorescence measurements, bolaform solutions of desired concentrations were prepared in Milli-Q water (18 MΩ·cm) and equilibrated overnight before measurement. For measurements of NPN fluorescence, a 10^{-3} M aqueous stock solution of the probe in Milli-Q water containing 1% (v/v) methanol was used. Solutions containing NPN (1×10^{-5} M) were excited at 340 nm, and the emission spectra were measured using excitation and emission slit widths of 5 and 10 nm, respectively. Fluorescence spectra of EB were recorded at the excitation wavelength 485 nm. The excitation and emission slit widths were 5 nm and 5−10 nm, respectively.

The steady-state fluorescence anisotropy of the DPH probe was measured on a JobinYvon Spex Fluorolog-3 spectrofluorometer equipped with a temperature-controlled cell holder. For anisotropy measurements, a stock solution of DPH (10^{-3} M) probe was prepared in super dry methanol, and the final DPH concentration in each sample was maintained at 1 μM. The sample was excited at 350 nm, and the emission was recorded at 450 nm using excitation and emission slit widths of 2.5 nm and 2.5−5 nm, respectively. The anisotropy was calculated by the software using the equation[51]

$$r = (I_{VV} - GI_{VH})/(I_{VV} + 2GI_{VH}) \qquad (1)$$

where I_{VV} and I_{VH} are the fluorescence intensities when the emission polarizer is oriented parallel and perpendicular, respectively, to the vertically oriented excitation polarizer, and G ($= I_{HV}/I_{HH}$) is the instrumental grating factor.

The measurements of time-resolved anisotropy decay of DPH in the presence of bolaforms were performed on an Optical Building Blocks Corporation Easylife instrument that uses a picosecond diode laser (380 nm, IBH, nanoLED-03) as the light source. The response time of this laser system was 100 ps. The measurements were carried out using the time-correlated single-photon counting method with the same samples employed for steady-state measurements. The fluorescence anisotropy decay was followed at 450 nm. The decay data were fit to the equation[51]

$$r(t) = (r_0 - r_\infty)e^{-t/\theta} + r_\infty \qquad (2)$$

where r_0 and r_∞ are the anisotropy of the DPH probe at $t = 0$ and ∞ time, respectively, and θ is rotational correlation time.

Isothermal Titration Calorimetry (ITC). ITC measurements were performed on a microcalorimeter (Microcal iTC$_{200}$). A concentrated (60 mM) stock solution of the respective bolaform was taken in a microsyringe of capacity 40 μL and added in multiple stages (2 μL for each injection) to Milli-Q water (160 μL) kept in the calorimeter cell of capacity 200 μL under constant stirring (400 rpm) condition. The stepwise heat of dilution of the bolaform solution was recorded. The reference cell was also filled with Milli-Q water. All measurements were performed twice at 25 °C to check reproducibility.

Dynamic Light Scattering. The measurements of hydrodynamic diameter (d_h) of aggregates in aqueous media were carried out on a dynamic light scattering (DLS) spectrometer (HORIBA Scientific nano partica NANO PARTICLE ANALYZER SZ-100, Kyoto, Japan) equipped with a DPSS Class I laser (λ_0 = 532 nm) operated at 10 mW. The scattering intensity was measured at an angle $\theta = 90°$ to the incident beam. Surfactant solutions were filtered into the cuvette using a Millipore Millex syringe filter (Triton-free, 0.22 μm). For all light scattering measurements, the sample was equilibrated at 25 °C for 10 min before the measurement. The data acquisition was carried out for at least 100 counts, and each experiment was repeated three times.

Atomic Force Microscopy (AFM). AFM measurements were conducted by a Nanoscope IIIA instrument from Digital Instruments

in tapping mode under ambient conditions. For the sample preparation, one drop of 20 mM bolaform solution was placed on a clean cover glass and spin-coated on an Advanced Spin Coating System (model no. EZspinADV) at 90 rpm speed. Before measurement, the sample was dried for at least 2 days in a vacuum desiccator.

DNA Binding Study. To determine the binding affinity of the investigated bolaforms with DNA, fluorescence quenching of the ct-DNA-EB complex was measured in the presence of varying concentrations of bolaforms. For fluorescence titration using the EB probe, a stock solution of EB (10 μM) in Milli-Q water was used. The calf thymus DNA (ct-DNA) stock solution (100 μg/mL) was prepared in Milli-Q water and stored under cooled conditions for further use. All sample solutions containing ct-DNA-EB and bolaform of desired concentrations were prepared in Milli-Q water (18 MΩ·cm) and equilibrated overnight before measurement. All measurements were carried out at room temperature (~25 °C).

***In Vitro* Transfection Assay.** Serum-free DMEM was used as a transfection material growth medium. Adherent cell Hek 293 and GFP VIVIT DNA were used for the transfection study. The ideal confluency for cells was between 70 and 90% at the time of transfection. The transfection protocol was based on a Thermo Fischer Scientific user guide. Briefly, 1 day before transfection, 2.0×10^4 cells per well were seeded in 200 μL of growth media. The GFP VIVIT plasmid DNA was diluted to 0.1 μg in 20 μL of serum-free DMEM. For the control experiment, 0.6 μL of the turbofectamine transfection agent was added to the vial of diluted plasmid DNA. The bola−DNA complexes formed by Bola-1 and Bola-2 were similarly produced with diluted plasmid DNA in various quantities in separate vials before transfection. Instantaneous vortexing was performed to prepare the vials, followed by a 15−20 min incubation period at ambient temperature. Each well received a dose of the transfection solution and plasmid DNA mixture in a dropwise manner. After the addition of the transfection reagent, the plate was gently rocked to ensure a uniform distribution of the complexes. Afterward, it was placed in a CO$_2$ incubator at 37 °C. Finally, with the help of immunofluorescence microscopy, transgene expression was examined after 24 h of incubation to assess transfection efficiency. The efficiency in a specific field was tested under a microscope by comparing fluorescence expression in GFP-expressed cells to unexpressed cells. A control set was kept, which was transfected with GFP VIVIT DNA by turbofecatamine and then compared with sample sets.

Cytotoxicity Assay. Among various methods, the MTT assay is a widely used colorimetric assay for assessing cytotoxicity. In this study, we performed the MTT assay according to the abcam protocol in the Hek 293 cell line to evaluate the cytotoxic potential of the cationic bolaforms. The bolaform was incubated in the cells for 6 h, followed by the MTT assay. The absorbance of the formazan dye was measured using a Cytation 5 multiple plate reader.

Antimicrobial Assay. Two bacterial strains, *S. aureus* and *E. coli* (DH5alpha), were used in the antimicrobial testing. Stock cultures were kept at 80 °C in a 20% glycerol solution. These two strains were inoculated into Luria−Bertani (LB) broth prior to studies, where they were cultured overnight at 37 °C. On the following day, 400 μL of the overnight culture was placed in 10 mL of sterile LB broth. For an antibacterial assay, an aliquot (200 μL) of *E. coli* was taken into each well of a 96-well plate, and the new culture was maintained at 37 °C with continuous shaking at 140 rpm on an orbital shaker. Bola-1 was diluted serially in the first five wells from 150 to 10 μM, while the sixth well was left undisturbed for a controlled experiment. *S. aureus* was aliquoted similarly in the following six wells, 200 μL in each. Bola-1 was added in accordance with the aforementioned terms. A similar protocol was followed in the case of Bola-2 as well for both Gram-positive and Gram-negative microorganisms. Finally, the plate was taken at intervals of 0, 240, and 1440 min, and the turbidity was measured at 600 nm through a Cytation 5 plate reader. The antimicrobial activity was assessed by investigating its ability to reduce bacterial growth (colony formation). The growth of bacteria was measured by monitoring changes in optical density, which was expressed in terms of colony forming unit (CFU). Following the same procedure, we conducted control tests on both species under two

conditions: without any antibiotic and in the presence of a recommended concentration of a well-established antibiotic. For *E. coli*, we used kanamycin at a concentration of 40 μg/mL (~82.6 μM) as described by Sulavik et al.[52] and for *S. aureus*, we used ampicillin at a concentration of 0.25 μg/mL (~0.7 μM).[53]

RESULTS AND DISCUSSION

Surface Activity. Surface tension (γ) of aqueous surfactant solutions is generally reduced with increasing surfactant concentration due to their surface-active properties. The γ *vs* log[Bola] plots of the bolaforms are depicted in Figure 2. The
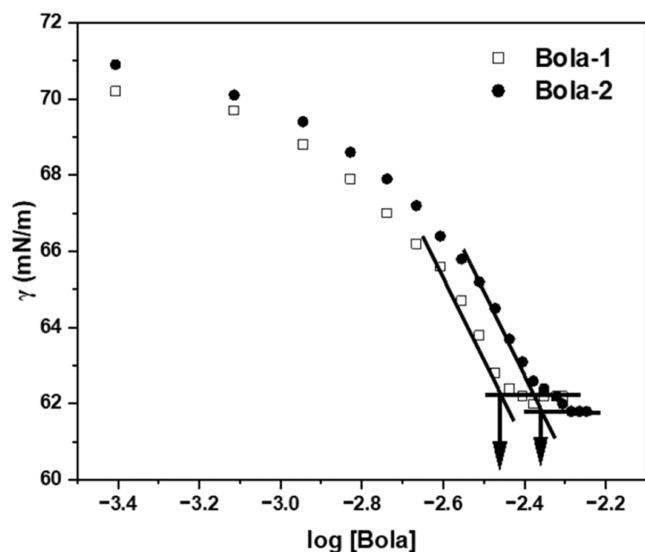

Figure 2. Surface tension (γ) *vs* log[Bola] plots for aqueous solutions (pH 6) of Bola-1 and Bola-2 at room temperature (~25 °C).

γ value of the aqueous solutions of Bola-1 and Bola-2 is found to decrease with an increase in [Bola]. However, due to the presence of two polar groups, bolaform surfactants exhibit less surface activity in comparison to conventional surfactants with only one headgroup in their structure. This is reflected by the higher γ_{cmc} values (~62 mN m^{-1}) in comparison to single-headed surfactants, which means that both Bola-1 and Bola-2 behave like electrolytes. The polar character of the bolaforms can be attributed to the presence of dihydroxyalkyl moiety in the head groups. Interestingly, however, the ST profile of both Bola-1 and Bola-2 exhibit a sharp break indicating aggregate formation above a critical concentration. This is in contrast to literature reports that bolaforms with less than 12 carbon atoms in the spacer usually play an electrolytic role and those with higher spacer length form micelles.[54] The concentration corresponding to the breakpoint as indicated by the downward arrow in Figure 2 was taken as the critical aggregation concentration (CAC), which is included in Table 1. The measured CAC values are much lower than the corresponding

single-headed cationic surfactant with a six-carbon hydrocarbon tail.[55] The aggregate formation by the bolaforms was confirmed by the results of conductivity and fluorescence probe experiments, as discussed below. Also, it should be noted that Bola-1 shows a slightly higher surface activity and has a lower CAC value compared to Bola-2. This may be due to the −OH functional group at the ammonium head groups.

Determination of CAC. As precise knowledge of the onset concentration (CAC) for aggregation is important in various applications, we attempted to determine the CAC. In order to determine the CAC of the cationic bolaforms, we carried out electrical conductivity (κ) measurements in aqueous solutions. The electrical conductivity of a charged particle depends on its charge and size, and it increases with an increase in the concentration of that charged particle. The conductivity of charged amphiphiles, however, initially increases rapidly with an increase in the concentration of the amphiphile, followed by a very small increase of κ value after the CAC, which usually is indicated by a breakpoint in the κ *vs* concentration plot.[56] Figure 3 shows plots of κ *vs* [Bola] for both Bola-1 and Bola-2.
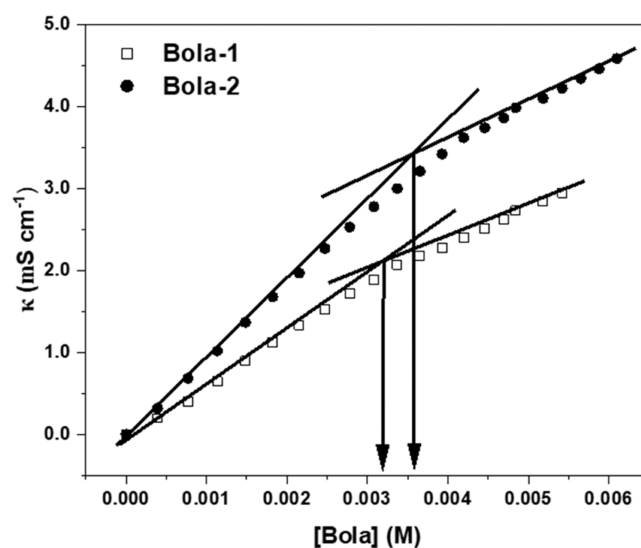
Figure 3. Electric conductivity (κ) *vs* [Bola] plots for aqueous solutions (pH 6) of Bola-1 and Bola-2 at 25 °C.

It can be found that the conductivity of the bolaforms is higher than those of conventional amphiphiles, which can be attributed to the presence of two cationic head groups in the structure of the bolaforms. A slightly lower value of κ in the case of Bola-2 must be due to its partial hydrolysis, producing corresponding singly charged species. However, the κ *vs* [Bola] plots of both bolaforms show a break indicating aggregate formation. The concentration corresponding to the breakpoint can be taken as the CAC value. The CAC values thus obtained from the corresponding plots are included in Table 1. As

Table 1. Values of Critical Aggregation Concentration (CAC) Obtained from Surface Tension (ST), Conductivity (Con), Fluorescence (Flu), Isothermal Titration Calorimetry (ITC), Degree of Counterion Dissociation (α), and Thermodynamic Properties ($\Delta_m G°$, $\Delta_m H°$, and $\Delta_m S°$) of Self-Assembly Formation by Bola-1 and Bola-2 in Water (pH 6) at 25 °C

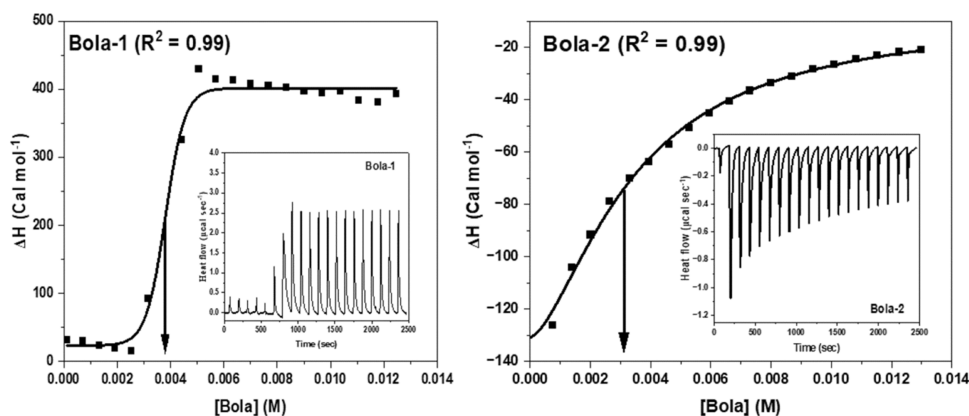|	CAC (mM)							
bolaform	Con (±0.2)	ST (±0.4)	Flu (±0.3)	ITC (±0.5)	α (±0.04)	$\Delta_m G°$ (±0.22) (kJ mol^{-1})	$\Delta_m H°$ (±0.1) (kJ mol^{-1})	$\Delta_m S°$ (±7.0) (J mol^{-1})
Bola-1	3.20	3.50	3.00	3.80	0.57	− 43.56	1.60	152.0
Bola-2	3.60	4.40	3.40	3.20	0.67	− 38.57	0.50	131.0

Figure 4. ITC titration curves and thermograms (inset) of (left) Bola-1 and (right) Bola-2 measured in water (pH 6) at 25 °C.

observed, the CAC value of Bola-1 is less than that of Bola-2. This is in contrast to what is expected. The combined effect of a smaller headgroup of Bola-2 and its partial ionization in water is expected to favor aggregate formation at a lower concentration due to the reduction of electrostatic repulsion between head groups. However, Bola-1 has a CAC value lower than that of Bola-2, which means the −OH functional groups in the cationic heads of Bola-1 have a favorable effect on aggregate formation. The effect of pK_a shift due to the aggregate formation cannot be ruled out. The intermolecular hydrogen-bonding interaction between head groups as well as with water molecules in the bulk may prevent water penetration into the aggregate structure, facilitating aggregate formation in the case of Bola-1.

The degree of micelle ionization (α) was calculated from the ratio of the slopes of the linear regions above and below the CAC in the respective κ vs [Bola] plot. The α-value can be used to measure the extent of the counterion binding to the micelles. The higher the value of α, the lower the counterion binding at the micelle surface. The larger α-value in the case of Bola-2 suggests a higher CAC and hence a lesser tendency to form aggregates. This is reflected in the values of molar Gibbs free energy change of aggregation ($\Delta_m G°$) per mole of the bolaforms as calculated from α-value using the equation[57]

$$\Delta_m G° = (3 - 2\alpha)RT \ln(\text{CAC}/55.5) - 2\alpha RT \ln 2$$
$$+ 2RT \ln 2 \qquad (3)$$

where CAC is in the molar unit. The $\Delta_m G°$ values for both bolaforms are listed in Table 1. As observed, the $\Delta_m G°$ value is moderately negative, which means that aggregation is thermodynamically favored for both bolaforms. The aggregate formation above a relatively lower CAC can be attributed to stronger 3-way intermolecular hydrogen-bonding interaction between urea linkages in the spacer chain. The existence of such hydrogen bonds in the neat sample is manifested by the lower stretching frequency of the >C=O group (amide I, 1644 cm^{-1}) and the broadening of the N−H stretching peak in the FT-IR spectrum of Bola-1 (Figure S1). The influence of bifurcated hydrogen bonding in the self-assembly of other amphiphilic molecules consisting of urea linkages has been reported in the literature.[58−60] A relatively higher negative $\Delta_m G°$ value for Bola-1 indicates that its aggregation is more favorable in comparison to Bola-2, which can be attributed to the presence of −OH functionality in the head groups of the former bolaform. This is also supported by the results (Table 1) of the ITC measurements, as discussed below.

Energetics of Self-Assembly Formation. Self-assembly of ionic surfactants depends upon electrostatic repulsions and hydrophobic interactions. The importance of these two factors can be obtained from the studies of the thermodynamic properties, such as the change of standard molar enthalpy ($\Delta_m H°$), entropy ($\Delta_m S°$), and Gibb's free energy ($\Delta_m G°$) of aggregation in which surfactant's alkyl chains, head groups, counterions, and the medium play vital roles. Thus, these thermodynamic parameters can give valuable insight into the principles that govern the formation of self-assembled aggregates. For conventional single-headed surfactants, it has been reported that the driving force for aggregation is the "hydrophobic effect". Thermodynamically, this means a positive entropy change in the system. Bola-1 and Bola-2 bolaforms not only have two cationic head groups but also have a relatively small hydrocarbon spacer chain containing two polar urea groups. This may make aggregation thermodynamically unfavorable. While conductivity measurements have suggested spontaneous aggregate formation by both Bola-1 and Bola-2, it is important to investigate the driving force for this process. Therefore, the energetics of micelle formation was studied by direct measurement of the $\Delta_m H°$ of micellization using isothermal titration calorimetry (ITC). The values of $\Delta_m H°$ and $\Delta_m G°$ enabled us to calculate the corresponding standard entropy change ($\Delta_m S°$) of micellization. The results of calorimetric titration are presented in Figure 4, and relevant data are collected in Table 1. The concentration corresponding to the inflection point (indicated by the downward arrow) of the titration curves was taken as the CAC. $\Delta_m H°$ values were obtained directly from the titration curves as the difference between heat changes at zero concentration and a concentration above CAC. The $\Delta_m H°$ value thus obtained is positive, suggesting that the micellization is endothermic. A relatively higher value of $\Delta_m H°$ for Bola-1 indicates a hydrogen-bonding interaction among bolaform molecules during self-assembly formation. The negative $\Delta_m G°$ value for both bolaforms confirms a thermodynamically favorable aggregate formation. This is also suggested by the positive $\Delta_m S°$ value obtained from the Gibbs−Helmholtz equation. However, it is important to note that the contribution of $\Delta_m H°$ is much less in comparison to the entropy term ($T\Delta S$) in the Gibbs−Helmholtz equation, suggesting that the self-assembly of both Bola-1 and Bola-2 is an entropy-driven process. The entropy-driven release of water molecules from the well-defined hydration shell of the bolaform molecules into bulk water outweighs the favorable
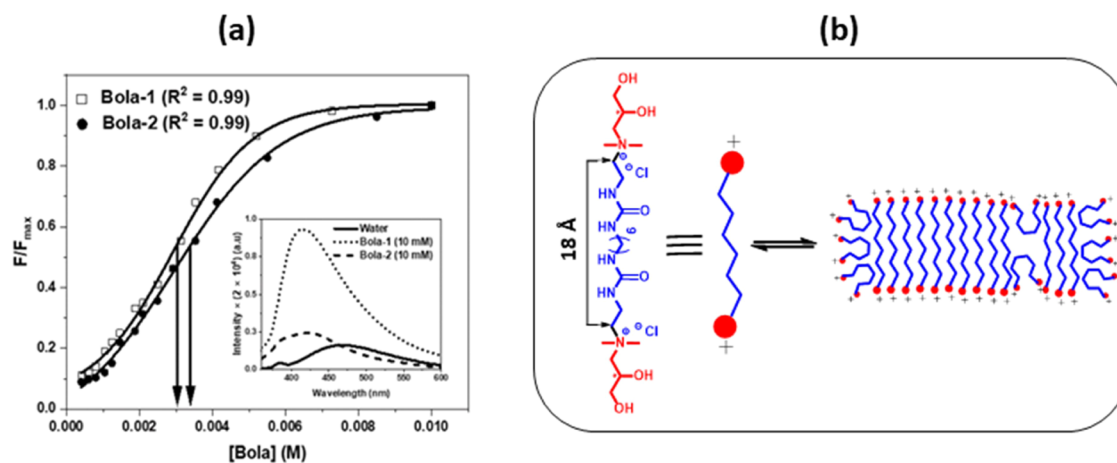
Figure 5. (a) Fluorescence titration curves for Bola-1 and Bola-2 in water (pH 6) at room temperature (~25 °C); inset: fluorescence spectra of NPN probe in aqueous solutions in the absence and presence of Bola-1 and Bola-2. (b) Cartoon picture showing possible aggregation behavior of Bola-1 and Bola-2.

enthalpy change due to the interaction between the hydrocarbon spacer. Thus, like conventional surfactants, the "hydrophobic effect" is the driving force for the self-assembly of Bola-1 and Bola-2 in water.

Fluorescence Probe Studies. Molecular self-assembly in water is a prominent area of research in chemical and biological sciences because the self-assembled aggregates in water have a potential application as nanocarriers of hydrophobic guest molecules. Fluorescence properties of molecules (probes) that are sensitive to changes in the environment have been used to detect and study the self-assembly of surfactants. Fluorescence probe studies can not only detect the formation of a self-assembled aggregate but also shed light on the nature of aggregates. Consequently, various types of fluorescent probe molecules have been employed by researchers. In the past, our group has successfully used NPN as a fluorescent probe for studying the self-assembly of surfactants in water.[61,62] Fluorescence spectrum of NPN has been found to exhibit a large spectral shift along with an enhancement of intensity upon incorporation into the hydrophobic microdomains of the self-assembled microstructures of surfactants. Therefore, NPN fluorescence was used to investigate the self-assembly of bolaforms in water. In the presence of Bola-1 or Bola-2, the relative fluorescence intensity (F/F_{max}, where F is the fluorescence intensities in the presence or absence of bolaform and F_{max} is the maximum intensity) of the NPN probe was observed to increase with the increase of [Bola] is shown in Figure 5a. A large blue shift of emission maximum (λ_{max}) of NPN can also be observed in the fluorescence spectra (see the inset of Figure 5a). The blue shift of λ_{max} and the enhancement of NPN fluorescence intensity suggest encapsulation of NPN molecules within the less polar environment of aggregates formed by self-assembly of the bolaform molecules in an aqueous solution. The sigmoidal feature of the fluorescence titration curves indicates a two-state process and suggests the existence of an equilibrium between bolaform monomers and self-assembled aggregates. The CAC values obtained from the inflection point (indicated by downward arrows in Figure 5a) of the fluorescence titration curves are listed in Table 1. The CAC values thus obtained are closely similar to the corresponding values obtained from ST and conductivity methods, which also indicate the accuracy of the measurements.

As observed from the fluorescence spectra, the blue shift is larger for Bola-1 (~60 nm) than for Bola-2 (~45 nm). Also, in the case of Bola-1, the enhancement of fluorescence intensity is larger in comparison to Bola-2. The rise of the fluorescence intensity signifies a viscous microenvironment around NPN molecules that are solubilized within the aggregates. The higher intensity rise and larger blue shift of the NPN fluorescence in the case of Bola-1 are indicative of a relatively less polar and more viscous microenvironment of NPN molecules in comparison to aggregates of Bola-2. This means that the hydrocarbon spacer chains are more tightly packed in the aggregates of Bola-1. As discussed earlier, this may be attributed to the −OH functional groups of the bolaform head groups, which prevent water penetration into the micellar core.

To further study the nature of the microenvironments of the aggregates, we performed steady-state as well as time-resolved fluorescence anisotropy (r) measurements using DPH as a probe molecule. Like NPN, the aqueous solution of the DPH probe also exhibits an enhancement of fluorescence intensity in the presence of Bola-1 and Bola-2 (see Figure S8), indicating solubilization of DPH molecules within less polar environments and thus confirming aggregate formation. The anisotropy decays are included in the SI (see Figures S9 and S10). The steady-state and time-resolved anisotropy data are summarized in Table 2. The r values of DPH in solutions of

Table 2. Values of Steady-State Fluorescence Anisotropy (r), Rotational Correlation Time (θ), and Microviscosity (η_m) of Bola-1 and Bola-2 in Aqueous Solution (pH 6) at Different Concentrations

bolaform	[Bola] (mM)	r	θ (ns)	η_m (mPa·s)
Bola-1	5.0	0.059 ± 0.002	0.82 ± 0.03	11.0 ± 0.2
	20.0	0.107 ± 0.005	1.16 ± 0.04	15.0 ± 0.8
Bola-2	5.0	0.043 ± 0.003	0.32 ± 0.05	4.0 ± 0.9
	20.0	0.082 ± 0.002	0.59 ± 0.02	8.0 ± 0.1

Bola-1 and Bola-2 are less than those of bilayer vesicles, which clearly indicates the fluid nature of the microenvironments of DPH molecules.[63] This is also substantiated by the lower values of microviscosity (η_m) calculated using rotational correlation time (θ) from the equation[51]
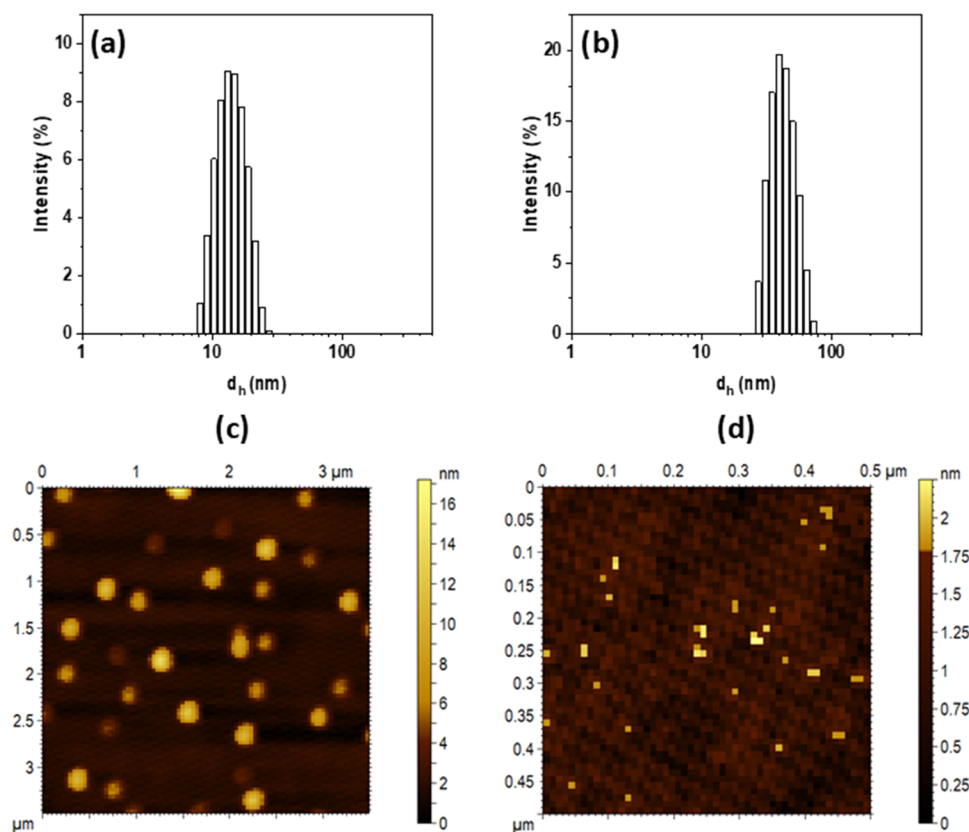
Figure 6. Hydrodynamic size (d_h) distribution histograms of aqueous solutions (20 mM, pH 6) of (a) Bola-1 and (b) Bola-2 at room temperature (~25 °C). AFM images of aqueous solutions (20 mM) of (c) Bola-1 and (d) Bola-2 at room temperature (~25 °C).

$$\eta_m = k_B T \theta / \nu \qquad (4)$$

where k_B is the Boltzmann constant, T is the absolute temperature, and ν is the molecular volume of the DPH (313 Å³)[63] probe. For both bolaforms, the η_m value is comparable to those of micellar aggregates of conventional surfactants but is less than that of bilayer vesicles.[63] Thus, the microviscosity data indicate the existence of micellar (spherical or cylindrical) aggregates in aqueous solutions of both bolaforms. However, the increase of the r or η_m value in going from dilute (5 mM) to concentrated (20 mM) solution suggests the growth of aggregates. As both Bola-1 and Bola-2 have shorter hydrophobic spacer which cannot bend, they are not expected to form vesicles or disks with bilayer membrane(s). However, the existence of monolayer vesicles (MVs) or monolayer disks cannot be ruled out. In such a case, the spacer chain of the bolaform molecules forming the monolayer membrane would be tightly packed due to strong intermolecular hydrogen-bonding interactions between adjacent urea groups, leading to the formation of rigid membrane with a higher η_m value. The more fluid microenvironments of DPH molecules indicate the formation of micellar aggregates. As the η_m value is much less than that of vesicular aggregates,[63] the shape of the micelles must be either spherical or cylindrical as shown in Figure 5b. This is supported by the results of DLS and AFM measurements, as discussed below.

Size and Shape of Aggregates. The measurement of the size of aggregates formed in the solution can give an idea of their shape. Therefore, we performed DLS measurements to estimate the mean hydrodynamic diameter (d_h) of the aggregates formed by the bolaforms in a 20 mM aqueous

solution. The size distribution histograms of both Bola-1 and Bola-2 are presented in Figure 6a,b. Both bolaforms exhibit aggregate formation with a relatively narrow size distribution. The mean hydrodynamic diameter of Bola-1 and Bola-2 was found to be ~15 and 40 nm, respectively. However, the molecular length of the bolaforms as obtained from molecular mechanics calculation using ChemDraw software (version) that uses MM2 force field is about 18 Å (see Figure 5b). Accordingly, if the bolaforms formed spherical micelles, the hydrodynamic diameter of aggregates of Bola-1 or Bola-2 would have been in the range of 2−3 nm. Thus, considering the length of the spacer chain, the aggregate size for both bolaforms is much larger than normal spherical micelles (3−5 nm),[64] which suggests that the bolaforms produce large elongated micelles as shown in Figure 5b.

The morphology of the aggregates was investigated by AFM measurements. The AFM images of 20 mM aqueous solutions of Bola-1 and Bola-2 are depicted in Figure 6c,d. As can be seen, the AFM image of Bola-1 exhibits the existence of large elongated aggregates of sizes in the range of 18−24 nm (see Figure 6c), which is closely similar to that of the mean d_h value obtained from DLS measurement. Interestingly, as observed in Figure 6d, Bola-2 exhibits the existence of rod-like micelles (see Figure 6d) with diameters in the range of 4−6 nm. This is, however, smaller than the mean d_h value obtained from the DLS measurements. This is expected because AFM measurements involved drying the samples.

DNA Binding Studies. The study of the binding of cationic surfactants to DNA has received huge attention because of its applications in DNA extraction, purification, counting, and transfection.[65] Various experimental methods,

including surface tension, fluorescence, isothermal titration calorimetry, and UV spectroscopy, have been employed in the past to study the interaction of DNA and cationic surfactants. DNA condensation is a fundamental process that has implications for gene delivery. Single-headed cationic surfactants with long hydrophobic chains can condense large DNA molecules into particles in the nanometer to micrometer size range.[66] Some researchers have suggested that the binding of cationic surfactants with DNA involves the formation of surfactant aggregates on the DNA when the surfactant concentration is above the CAC and subsequently the aggregates associated with the phosphate groups of DNA.[67] On the other hand, other groups of scientists think that a single surfactant monomer interacts with DNA solely through charge—charge interactions and subsequently catalyzes the binding of additional molecules.[68] Long-chain cationic surfactants could have their hydrocarbon tails pointing away from the DNA surface, which could promote intermolecular interactions between hydrophobic chains and thus favor DNA condensation. But short-chain surfactants that do not induce any condensation lie down on the DNA surface and directly interact with the DNA grooves through hydrophobic—hydrophobic interactions. However, still there is debate about the interaction of DNA with cationic surfactants.

To understand the driving forces involved in molecular interactions and the mode of binding, we investigated the complexation ability of Bola-1 and Bola-2 with DNA through measurements of fluorescence quenching of calf thymus DNA (ct-DNA)-bound ethidium bromide (EB). Although EB is weakly fluorescent in water, in the presence of DNA, the fluorescence intensity is greatly enhanced.[69] This has been associated with the intercalation of EB molecules between the base pairs of the DNA double helix. If an additive also occupies the same location occupied by EB molecules in the interaction with DNA, EB molecules are separated from DNA through a competitive binding process. This results in the fluorescence quenching of EB.

The fluorescence spectra of EB (1 μM) and the ct-DNA-EB complex designated as DNA in the absence and presence of Bola-1 and Bola-2 are depicted in Figure S11. It is seen that EB has a weakly intense peak in the absence of ct-DNA. But in the presence of ct-DNA, the fluorescence intensity increased remarkably. Also, as expected, the spectrum is red-shifted upon binding to the ct-DNA. Interestingly, upon the addition of Bola-1 or Bola-2, the fluorescence intensity of the ct-DNA-EB complex decreased with increasing concentration of the respective bolaform. The sigmoidal fit (Figure 7, inset) of the experimental data indicates a two-state equilibrium, and the extent of fluorescence quenching is much greater for Bola-1 in comparison to Bola-2. In other words, the binding of Bola-1 with ct-DNA is stronger than Bola-2. This is substantiated by the values of binding constants (K_b) estimated using the Stern—Volmer equation[51]

$$F_o/F = 1 + K_b[\text{Bola}] \tag{5}$$

where F_o and F are fluorescence intensities in the absence and presence of bolaform, respectively, and [Bola] is the bolaform concentration in mol L^{-1}. The Stern—Volmer plots (F_o/F vs [Bola]) are shown in Figure 7. A good fit of the experimental data to eq 5 suggests that the binding of cationic bolaforms to DNA involves a two-state equilibrium. However, the binding process involves an electrostatic interaction not only with an isolated negatively charged phosphate group on the DNA
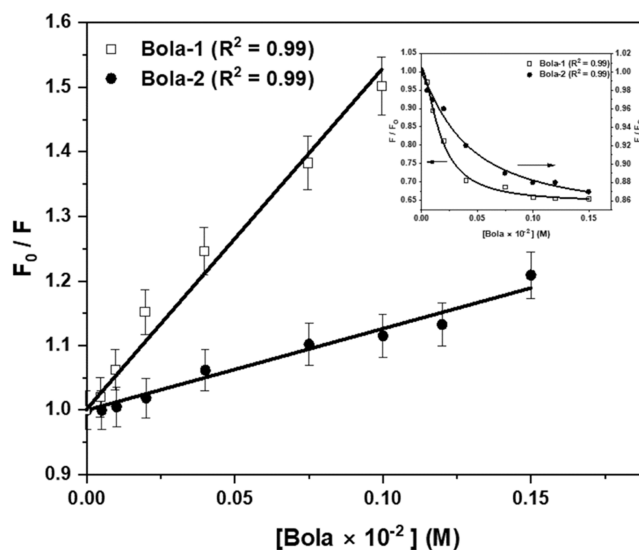

Figure 7. Stern—Volmer plots for fluorescence quenching of EB-DNA complex by Bola-1 and Bola-2 in water (pH 6) at room temperature (~25 °C); inset: fluorescence titration of EB-DNA complex for Bola-1 and Bola-2. The error bars show the standard deviation ($\pm$SD) from three separate measurements (n = 3).

strand but also through the hydrophobic spacer that lays on the DNA surface. The structural change (twisting) caused by the binding process pushes the EB molecules out of the DNA structure, resulting in its fluorescence quenching. The results suggest that Bola-1 has a higher complexation ability with ct-DNA in comparison to Bola-2. But unlike conventional cationic surfactants, no significant hydrophobic interactions between DNA and surfactant alkyl chains occur in the case of Bola-1 and Bola-2. This is consistent with the electrolytic nature of the bolaforms, as discussed earlier. The binding constant was calculated from the slope of the respective binding isotherm, and the K_b value of Bola-1 (521.34 $\pm$ 20.08 L mol^{-1}) was found to be much higher than that of Bola-2 (126.23 $\pm$ 5.37 L mol^{-1}). This means that Bola-1 is more effective in binding to DNA compared to Bola-2 that has no —OH groups at the cationic heads. Since both bolaforms have the same spacer length, the difference in DNA binding abilities must be associated with electrostatic interactions involving cationic head groups. This means that the —OH functional groups at the bolaform heads influence the binding phenomenon and are involved in hydrogen-bonding interactions with phosphate groups of DNA strands.

Gene Transfection Study. The limitations, such as host immune and inflammatory reactions, expense of production, the size limit of the exogenous DNA, and the risks of inducing tumorigenic mutations, have led researchers to find more efficient nonviral vectors. Despite the numerous studies[70] on the structure—activity relationship of cationic surfactants used in gene delivery, no solid conclusion is obtained due to the complexity of the transfection pathway. The transfection efficiency can be affected by variations in the hydrophilic headgroup structure, such as the charge density and orientation concerning the backbone. Thus, in the past, the focus of research has been the relationships between the degree of hydration of the cationic headgroup and the transfection efficiency and/or between the charge density of the headgroup and the transfection efficiency.[71]
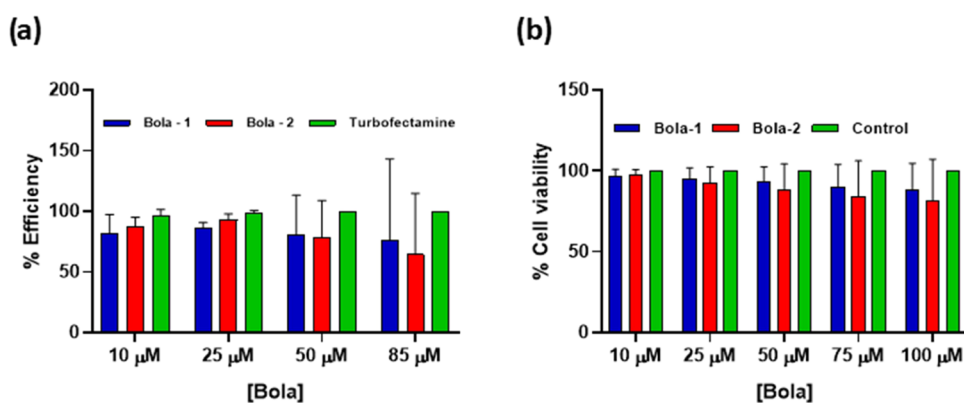
Figure 8. (a) Bar graphs showing gene transfection efficiency (%) of Bola-1 and Bola-2 at different concentrations with respect to turbofectamine. (b) Bar graphs showing cell viability (%) in the presence of Bola-1 and Bola-2 at different concentrations. The error bars show the standard deviation (±SD) from three separate measurements (n = 3).
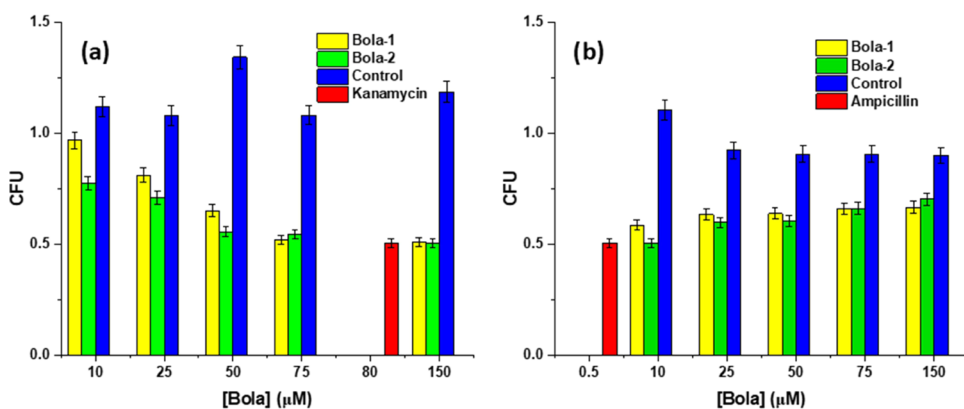

Figure 9. Bar graphs showing the antibacterial activity (CFU) of Bola-1 and Bola-2 (a) against *E. coli* and (b) against *S. aureus* microorganisms after 24 h. The error bars show the standard deviation (±SD) from three separate measurements (n = 3).

Therefore, to understand the structure−activity relationship, we have compared gene transfection efficiencies of Bola-1 and Bola-2. To study gene transfection efficiency, Bola-1 and Bola-2 were utilized at doses of 10, 25, 50, and 85 μM, with turbofectamine serving as the control. The results are summarized in Figure 8a. As observed, Bola-1 shows a gradual increase in transfection efficiency with increasing concentration from 10 to 85 μM. On the other hand, Bola-2 exhibits slightly higher transfection efficiency compared to Bola-1 at 10 and 25 μM, but the effectiveness decreased at higher concentrations. Thus, both Bola-1 and Bola-2 show a comparable transfection efficiency in comparison to the turbofectamine standard. However, the slightly lower gene transfection ability of Bola-1 may be associated with its stronger binding to the DNA chain. Thus, both Bola-1 and Bola-2 can be used as potential transfecting agents.

Cytotoxicity Studies. Cytotoxicity assessment is a crucial parameter for evaluating the potential of drugs to induce cell death. Many authors have reported favorable safety profiles of bolaforms justifying their use in biomedical applications. Considering the diversity of bolaform structures and their complex self-assembly behavior that can alter their mode of action, safety should be evaluated and not assumed. Indeed, the relationship between the cationic lipid structure and toxicity in gene delivery is very important. The charge density as well as the orientation of the hydrophilic headgroup can affect the toxicity of cationic surfactants. Thus, in this work, we have examined *in vitro* cytotoxicity of Bola-1 and Bola-2 using

an MTT assay. The results are presented in Figure 8b. It can be found that in both Bola-1 and Bola-2 at lower concentrations, the toxicity of both molecules is quite minimal and does not significantly affect cell viability. However, both amphiphiles exhibit some level of toxicity at higher concentrations (>75 μM). Despite their toxicity at higher concentrations, Bola-1 and Bola-2 can still be used as successful transfection agents at lower concentrations. This finding highlights the importance of careful dosage and concentration selection when using bolaamphiphiles as transfection agents. It is crucial to strike a balance between achieving effective transfection and minimizing cytotoxicity.

Antibacterial Activity. As the bacterial membrane is negatively charged, these cationic bolaforms can potentially disrupt or destabilize cell membranes by the initial electrostatic interaction. Since *in vitro* cytotoxicity measurements indicated significant toxicity of the bolaforms at concentrations greater than 75 μM, both Bola-1 and Bola-2 can act as effective antimicrobials at higher concentrations. The length of the hydrophobic spacer and the nature of the cationic head groups are important factors in determining antibacterial activity. Therefore, the antimicrobial activity studies were performed using both Gram-positive (*S. aureus*) and Gram-negative (*E. coli*) microorganisms as a model. *E. coli* is one of the most studied[72] microorganisms with a variety of pathogenic strains causing a range of negative health problems through foodborne contamination. On the other hand, *S. aureus* is a high-key human nosocomial as well as a foodborne pathogen.[73] To

assess the potential antimicrobial activity, we measured the survival of *E. coli* and *S. aureus* after exposure to the presence or absence of 10−150 μM bolaforms under aqueous conditions. We monitored the effects of these two compounds, Bola-1 and Bola-2, on the mentioned species at different concentrations and time intervals. The data are collected in Table S1 (see SI) and the data after 24 h are presented in Figure 9a,b. The data for the standard antibiotics are also included in the figure. As seen, after 24 h, Bola-1 and Bola-2 have a minimum inhibitory concentration (MIC) of 75 and 50 μM, respectively, for Gram-negative bacteria, which is less than that of kanamycin (∼82.6 μM).[52] Interestingly, both Bola-1 and Bola-2 demonstrated closely similar antibacterial activity with the MIC value of 10 μM in the case of Gram-positive bacteria, which is higher than that of ampicillin (∼0.7 μM).[53] This means that, in comparison to kanamycin, Bola-1 and Bola-2 are more effective antibacterial agents for Gram-negative bacteria. However, in comparison to ampicillin, Bola-1 and Bola-2 are less effective antibacterial agents for Gram-positive bacteria.

CONCLUSIONS

In summary, two novel bolaforms, Bola-1 and Bola-2, were designed and developed, which were found to be weakly surface-active, reflecting their more electrolytic nature. Despite the bipolar structure, the bolaforms were observed to self-assemble to form elongated micelles in water above a relatively low CAC value, which is less than that of traditional single-headed cationic surfactants with comparable hydrocarbon chain lengths. Indeed, the self-assembly formation by the bolaforms is thermodynamically more favorable than corresponding single-headed cationic surfactants. Further, these bolaforms also follow thermodynamic principles of self-assembly similar to those of classical surfactants. That is like traditional surfactants, the self-assembly of both Bola-1 and Bola-2 is an entropy-driven process. However, unlike typical symmetrical bolaamphiphiles, the driving force for aggregation is higher than corresponding single-headed amphiphiles. The favorable aggregation in the cases of Bola-1 and Bola-2 is due to the existence of urea groups in the spacer chain. The bolaforms investigated in this work strongly bind to ct-DNA through electrostatic interactions at concentrations much lower than their CAC value and lie on the DNA surface. Bola-1 exhibits stronger binding to DNA due to the hydrogen-bonding interactions of the multiple hydroxyl groups at the cationic heads. Despite stronger interaction with DNA molecules, the transfection efficiency of Bola-1 was observed to be similar to that of Bola-2. In contrast to literature reports, the hydroxyl groups at the cationic heads have no role in DNA transfection. Also, the transfection efficiency of both Bola-1 and Bola-2 was found to be comparable to that of the turbofectamine standard at low concentrations. This means that both Bola-1 and Bola-2 can be used as potential transfecting agents. Interestingly, both Bola-1 and Bola-2 have low cytotoxicity against the HEK 293 cell line. The bolaforms were found to have better antibacterial activity against *E. coli* in comparison to kanamycin antibiotic but less activity against *S. aureus* than ampicillin antibiotic. Thus, the bolaforms investigated in this work can find applications in areas such as gene delivery and antimicrobials.

ASSOCIATED CONTENT

ⓢ Supporting Information

The Supporting Information is available free of charge at https://pubs.acs.org/doi/10.1021/acs.langmuir.3c00885.

> Details of synthetic procedure, chemical identification of the synthesized bolaamphiphiles, FT-IR, ^{1}H and ^{13}C NMR spectra, HRMS spectra, representative time-resolved anisotropy decay plots, the fluorescence emission spectra of DPH, EB, and ct-DNA-EB comple (PDF)

AUTHOR INFORMATION

Corresponding Author

Joykrishna Dey − *Department of Chemistry, Indian Institute of Technology Kharagpur, Kharagpur 721302, India;* orcid.org/0000-0001-8357-5560; Email: joydey@chem.iitkgp.ac.in

Authors

Pabitra Mondal − *Department of Chemistry, Indian Institute of Technology Kharagpur, Kharagpur 721302, India*

Sadhana Roy − *Department of Biotechnology, Indian Institute of Technology Kharagpur, Kharagpur 721302, India*

Somdeb Bose Dasgupta − *Department of Biotechnology, Indian Institute of Technology Kharagpur, Kharagpur 721302, India*

Complete contact information is available at:
https://pubs.acs.org/10.1021/acs.langmuir.3c00885

Notes

The authors declare no competing financial interest.

REFERENCES

(1) Fuhrhop, J. H.; Wang, T. Bolaamphiphiles. *Chem. Rev.* **2004**, *104*, 2901−2937.

(2) Kunitake, T.; Kunitake, Y.; Kunitake, M.; Yasunami, S.; Takarabe, K. Formation of Stable Bilayer Assemblies in Water from Single-Chain Amphiphiles. Relationship between the Amphiphile Structure and the Aggregate Morphology. *J. Am. Chem. Soc.* **1981**, *103*, 5401−5413.

(3) Liu, Y.; Wang, T.; Huan, Y.; Li, Z.; He, G.; Liu, M. Self-assembled supramolecular nanotube yarn. *Adv. Mater.* **2013**, *25*, 5875−5879.

(4) Cheng, X.; Liu, F.; Zeng, X.; Ungar, G.; Kain, J.; Diele, S.; Prehm, M.; Tschierske, C. Influence of Flexible Spacers on Liquid-Crystalline Self-Assembly of T-Shaped Bolaamphiphiles. *J. Am. Chem. Soc.* **2011**, *133*, 7872−7881.

(5) Shimizu, T.; Kameta, N.; Ding, W.; Masuda, M. Supramolecular Self-Assembly into Biofunctional Soft Nanotubes: From Bilayers to Monolayers. *Langmuir* **2016**, *32*, 12242−12264.

(6) Xia, Y.; Dong, L.; Jin, Y.; Wang, S.; Yan, L.; Yin, S.; Zhou, S.; Song, B. Water-soluble nano-fluorogens fabricated by self-assembly of

bolaamphiphiles bearing AIE moieties: towards application in cell imaging. *J. Mater. Chem. B* **2015**, *3*, 491–497.

(7) Zeng, X.; Prehm, M.; Ungar, G.; Tschierske, C.; Liu, F. Formation of a Double Diamond Cubic Phase by Thermotropic Liquid Crystalline Self-Assembly of Bundled Bolaamphiphiles. *Angew. Chem., Int. Ed.* **2016**, *55*, 8324–8327.

(8) Chen, C.; Wang, T.; Fu, Y.; Liu, M. trans-cis Configuration regulated supramolecular polymer gels and chirality transfer based on a bolaamphiphilic histidine and dicarboxylic acids. *Chem. Commun.* **2016**, *52*, 1381–1384.

(9) Yuan, C.; Jiang, J.; Sun, H.; Wang, D.; Hu, Y.; Liu, M. Opposite Enantioselectivity by Nanotubes and Nanospheres Self-Assembled from Dirhodium(II) and an L-Glutamic Acid Terminated Bolaamphiphile. *ChemCatChem* **2018**, *10*, 2190–2194.

(10) Zhao, Y.; Yang, W.; Wang, D.; Wang, J.; Li, Z.; Hu, X.; King, S.; Rogers, S.; Lu, J. R.; Xu, H. Controlling the diameters of nanotubes self-assembled from designed peptide bolaphiles. *Small* **2018**, *14*, No. 1703216.

(11) Zeng, H.; Johnson, M. E.; Oldenhuis, N. J.; Tiambeng, T. N.; Guan, Z. Structure-based design of dendritic peptide bolaamphiphiles for siRNA delivery. *ACS Cent. Sci.* **2015**, *1*, 303–312.

(12) Jiang, J.; Meng, Y.; Zhang, L.; Liu, M. Self-Assembled Single-Walled Metal-Helical Nanotube (M-HN): Creation of Efficient Supramolecular Catalysts for Asymmetric Reaction. *J. Am. Chem. Soc.* **2016**, *138*, 15629–15635.

(13) Zhou, C.; Feng, X.; Wang, R.; Yang, G.; Wang, T.; Jiang, J. Hierarchical Assembly of L-Phenylalanine-Terminated Bolaamphiphile with Porphyrin Show Tunable Nanostructures and Photocatalytic Properties. *ACS Omega* **2018**, *3*, 10638–10646.

(14) Kim, M. C.; Lee, S. Y. Peroxidase-like oxidative activity of a manganese-coordinated histidyl bolaamphiphile self-assembly. *Nanoscale* **2015**, *7*, 17063–17070.

(15) Kwak, J.; Kim, M. C.; Lee, S. Y. An enzyme-coupled artificial photosynthesis system prepared from antenna protein-mimetic tyrosyl bolaamphiphile self-assembly. *Nanoscale* **2016**, *8*, 15064–15070.

(16) Lee, C.; Lee, S. Y. Hemin-bound cysteinyl bolaamphiphile self-assembly as a horseradish peroxidase-mimetic catalyst. *RSC Adv.* **2017**, *7*, 38989–38997.

(17) Meister, A.; Blume, A. Self-assembly of bipolar amphiphiles. *Curr. Opin. Colloid Interface Sci.* **2007**, *12*, 138–147.

(18) Benvegnu, T.; Brard, M.; Plusquellec, D. Archaeabacteria bipolar lipid analogues: structure, synthesis and lyotropic properties. *Curr. Opin. Colloid Interface Sci.* **2004**, *8*, 469–479.

(19) Roussel, M.; Lognone, V.; Plusquellec, D.; Benvegnu, T. Monolayer lipid membrane-forming dissymmetrical bolaamphiphiles derived from alginate oligosaccharides. *Chem. Commun.* **2006**, 3622–3624.

(20) Popov, M.; Linder, C.; Deckelbaum, R. J.; Grinberg, S.; Hansen, I. H.; Shaubi, E.; Waner, T.; Heldman, E. Cationic vesicles from novel bolaamphiphilic compounds. *J. Liposome Res.* **2010**, *20*, 147–159.

(21) Popov, M.; Grinberg, S.; Linder, C.; Waner, T.; Levi-Hevroni, B.; Deckelbaum, R. J.; Heldman, E. Site-directed decapsulation of bolaamphiphilic vesicles with enzymatic cleavable surface groups. *J. Controlled Release* **2012**, *160*, 306–314.

(22) Popov, M. Nano-Sized Vesicles Made of Monolayered Membranes for Targeted Drug Delivery. Ph.D. Thesis, Ben-Gurion University of the Negev, Israel, 2010.

(23) Grinberg, S.; Kipnis, N.; Linder, C.; Kolot, V.; Heldman, E. Asymmetric bolaamphiphiles from vernonia oil designed for drug delivery. *Eur. J. Lipid Sci. Technol.* **2010**, *112*, 137–151.

(24) Grinberg, S.; Kolot, V.; Linder, C.; Shaubi, E.; Kas'yanov, V.; Deckelbaum, R. J.; Heldman, E. Synthesis of novel cationic bolaamphiphiles from vernonia oil and their aggregated structures. *Chem. Phys. Lipids* **2008**, *153*, 85–97.

(25) Wu, G.; Thomas, J.; Smet, M.; Wang, Z.; Zhang, X. Controlling the self-assembly of cationic bolaamphiphiles: hydrotropic counteranions determine aggregated structures. *Chem. Sci.* **2014**, *5*, 3267–3274.

(26) Gliozzi, A.; Relini, A.; Chong, P. L.-G. Structure and permeability properties of biomimetic membranes of bolaform archaeal tetraether lipids. *J. Membr. Sci.* **2002**, *206*, 131–147.

(27) Wiesman, Z.; Dom, N. B.; Sharvit, E.; Grinberg, S.; Linder, C.; Heldman, E.; Zaccai, M. Novel cationic vesicle platform derived from vernonia oil for efficient delivery of DNA through plant cuticle membranes. *J. Biotechnol.* **2007**, *130*, 85–94.

(28) Grinberg, S.; Linder, C.; Kolot, V.; Waner, T.; Wiesman, Z.; Shaubi, E.; Heldman, E. Novel cationic amphiphilic derivatives from vernonia oil: synthesis and self-aggregation into bilayer vesicles, nanoparticles, and DNA complexants. *Langmuir* **2005**, *21*, 7638–7645.

(29) Denoyelle, S.; Polidori, A.; Brunelle, M.; Vuillaume, P. Y.; Laurent, S.; ElAzhary, Y.; Pucci, B. Synthesis and preliminary biological studies of hemifluorinated bifunctional bolaamphiphiles designed for gene delivery. *New J. Chem.* **2006**, *30*, 629–646.

(30) Eaton, M. A. W.; Baker, T. S.; Catterall, C. F.; Crook, K.; Macaulay, G. S.; Mason, B.; J Norman, T.; Parker, D.; Perry, J. J. B.; Taylor, R. J.; Turner, A.; Weir, A. N. A New Self-Assembling System for Targeted Gene Deliver. *Angew. Chem., Int. Ed.* **2000**, *112*, 4229–4233.

(31) D'Souza, G. G. M.; Boddapati, S. V.; Weissig, V. Mitochondrial leader sequence-plasmid DNA conjugates delivered into mammalian cells by DQAsomes co-localize with mitochondria. *Mitochondrion* **2005**, *5*, 352–358.

(32) Lainé, C.; Mornet, E.; Lemiègre, L.; Montier, T.; Cammas-Marion, S.; Neveu, C.; Carmoy, N.; Lehn, P.; Benvegnu, T. Folate-Equipped Pegylated Archaeal Lipid Derivatives: Synthesis and Transfection Properties. *Chem. - Eur. J.* **2008**, *14*, 8330–8340.

(33) Chen, J.-X.; Xu, X.-D.; Yang, S.; Yang, J.; Zhuo, R.-X.; Zhang, X.-Z. Self-Assembled BolA-like Amphiphilic Peptides as Viral-Mimetic Gene Vectors for Cancer Cell Targeted Gene Delivery. *Macromol. Biosci.* **2013**, *13*, 84–92.

(34) Cho, D. Y.; Cho, H.; Kwon, K.; Yu, M.; Lee, E.; Huh, K. M.; Lee, D. H.; Kang, H. Triphenylphosphonium-Conjugated Poly(ϵ-caprolactone)- Based Self-Assembled Nanostructures as Nanosized Drugs and Drug Delivery Carriers for Mitochondria-Targeting Synergistic Anticancer Drug Delivery. *Adv. Funct. Mater.* **2015**, *25*, 5479–5491.

(35) Gupta, K.; Afonin, K. A.; Viard, M.; Herrero, V.; Kasprzak, W.; Kagiampakis, I.; Kim, T.; Koyfman, A. Y.; Puri, A.; Stepler, M.; Sappe, A.; KewalRamani, V. N.; Grinberg, S.; Linder, C.; Heldman, E.; Blumenthal, R.; Shapiro, B. A. Bolaamphiphiles as carriers for siRNA delivery: From chemical syntheses to practical applications. *J. Controlled Release* **2015**, *213*, 142–151.

(36) Fenart, L.; Casanova, A.; Dehouck, B.; Duhem, C.; Slupek, S.; Cecchelli, R.; Betbeder, D. Evaluation of effect of charge and lipid coating on ability of 60-nm nanoparticles to cross an in vitro model of the blood–brain barrier. *J. Pharmacol. Exp. Ther.* **1999**, *291*, 1017–1022.

(37) Dakwar, G. R.; Hammad, I. A.; Popov, M.; Linder, C.; Grinberg, S.; Heldman, E.; Stepensky, D. Delivery of proteins to the brain by bolaamphiphilic nano-sized vesicles. *J. Controlled Release* **2012**, *160*, 315–321.

(38) Popov, M.; Hammada, I. A.; Bachar, T.; Grinberg, S.; Linder, C.; Stepensky, D.; Heldman, E. Delivery of analgesic peptides to the brain by nano-sized bolaamphiphilic vesicles made of monolayer membranes. *Eur. J. Pharm. Biopharm.* **2013**, *85*, 381–389.

(39) Fichert, T.; Regelin, A.; Massing, U. Synthesis and transfection properties of novel non-toxic monocationic lipids. Variation of lipid anchor, spacer and head group structure. *Bioorg. Med. Chem. Lett.* **2000**, *10* (8), 787–791.

(40) Ananta Laxmi, A.; Vijayalakshmi, P.; Kaimal, T. N.; Chaudhuri, A.; Ramadas, Y.; Rao, N. M. Novel non-glycerol-based cytofectins with lactic acid-derived head groups. *Biochem. Biophys. Res. Commun.* **2001**, *289* (5), 1057–1062.

(41) Banerjee, R.; Mahidhar, Y. V.; Chaudhuri, A.; Gopal, V.; Rao, N. M. Design, synthesis, and transfection biology of novel cationic

glycolipids for use in liposomal gene delivery. *J. Med. Chem.* **2001**, *44* (24), 4176−4185.

(42) Mukherjee, K.; Bhattacharyya, J.; Sen, J.; Sistla, R.; Chaudhuri, A. Covalent grafting of common trihydroxymethylaminomethane in the headgroup region imparts high serum compatibility and mouse lung transfection property to cationic amphiphile. *J. Med. Chem.* **2008**, *51* (6), 1967−1971.

(43) Mahidhar, Y. V.; Rajesh, M.; Madhavendra, S. S.; Chaudhuri, A. Distance of hydroxyl functionality from the quaternized center influence DNA binding and in vitro gene delivery efficacies of cationic lipids with hydroxyalkyl headgroups. *J. Med. Chem.* **2004**, *47* (23), 5721−5728.

(44) Mahidhar, Y. V.; Rajesh, M.; Chaudhuri, A. Spacer-arm modulated gene delivery efficacy of novel cationic glycolipids: design, synthesis, and in vitro transfection biology. *J. Med. Chem.* **2004**, *47* (16), 3938−3948.

(45) van Esch, J. H.; Schoonbeek, F.; de Loos, M.; Kooijman, H.; Spek, A. L.; Kellogg, R. M.; Feringa, B. L. Cyclic bis-urea compounds as gelators for organic solvents. *Chem. - Eur. J.* **1999**, *5*, 937−950.

(46) Estroff, L. A.; Hamilton, A. D. Effective Gelation of Water Using a Series of Bis-urea Dicarboxylic Acids. *Angew. Chem., Int. Ed.* **2000**, *39*, 3447−3450.

(47) Jagtap, A. D.; Kondekar, N. B.; Sadani, A. A.; Chern, J. W. Ureas: applications in drug design. *Curr. Med. Chem.* **2017**, *24*, 622−651.

(48) Ghosh, A. K.; Brindisi, M. Urea Derivatives in Modern Drug Discovery and Medicinal Chemistry. *J. Med. Chem.* **2020**, *63*, 2751−2788.

(49) Pal, A.; Dey, J. Gelation of organic solvents by N-(n-tetradecylcarbamoyl)-L-amino acids. *Supramol. Chem.* **2015**, *27*, 127−135.

(50) Pal, A.; Dey, J. L-Cysteine-derived Ambidextrous Gelators of Aromatic Solvents and Ethanol/Water Mixtures. *Langmuir* **2013**, *29*, 2120−2127.

(51) Lakowicz, J. R. *Principles of Fluorescence Spectroscopy*; Plenum Press: New York, 1983.

(52) Sulavik, M. C.; Houseweart, C.; Cramer, C.; Jiwani, N.; Murgolo, N.; Greene, J.; Didomenico, B.; Shaw, K. J.; Miller, G. H.; Hare, R.; Shimeri, G. Aantibiotic Susceptibility Profiles of *Escherichia coli* Strains Lacking Multidrug Efflux Pump Genes. *Antimicrob. Agents Chemother.* **2001**, *45*, 1126−1136.

(53) Pengov, A.; Ceru, S. Antimicrobial Drug Susceptibility of *Staphylococcus aureus* Strains Isolated from Bovine and Ovine Mammary Glands. *J. Dairy Sci.* **2003**, *86*, 3157−3163.

(54) Nuraje, N.; Baib, H.; Suc, K. Bolaamphiphilic molecules: Assembly and applications. *Prog. Polym. Sci.* **2013**, *38*, 302−343.

(55) Maiti, K.; Mitra, D.; Mitra, R. N.; Panda, A. K.; das, P. K.; Rakshit, A. K.; Moulik, S. P. Self-aggregation of synthesized bolaforms and their mixtures with sodium dodecyl sulfate (SDS) and cetyltrimethylammonium bromide (CTAB) in aqueous medium. *J. Phys. Chem. B* **2010**, *114*, 7499−7508.

(56) Song, Y.; Sun, R.; Zhao, K.; Pan, X.; Zhou, H.; Li, D. An induction current method for determining the critical micelle concentration and the polarity of surfactants. *Colloid Polym. Sci.* **2015**, *293*, 1525−1534.

(57) Zana, R. Critical Micellization Concentration of Surfactants in Aqueous Solution and Free Energy of Micellization. *Langmuir* **1996**, *12*, 1208−1211.

(58) Pal, A.; Mahapatra, R. D.; Dey, J. Understanding the Role of H-Bonding in Self-Aggregation in Organic Liquids by Fatty Acid Amphiphiles with a Hydrocarbon Tail Containing Different H-Bonding Linker Groups. *Langmuir* **2014**, *30* (46), 13791−13798.

(59) Gong, X.; Sagnella, S.; Drummond, C. J. Nanostructured self-assembly materials formed by non-ionic urea amphiphiles. *Int. J. Nanotechnol.* **2008**, *5*, 370−392.

(60) Vos, M. R. J.; Jardĺ, G. E.; Pallas, A. L.; Breurken, M.; van Asselen, O. L. J.; Bomans, P. H. H.; Leclère, P. E. L. G.; Frederik, P. M.; Nolte, R. J. M.; Sommerdijk, N. A. J. M. The bis-urea motif as a

tool to functionalize self-assembled nanoribbons. *J. Am. Chem. Soc.* **2005**, *127*, 16768−16769.

(61) Ghosh, R.; Dey, J. Vesicle-to-Micelle Transition in Aqueous Solutions of L-Cysteine- Derived Carboxylate Surfactants Containing Both Hydrocarbon and Poly(ethylene glycol) Tails. *Langmuir* **2017**, *33*, 543−552.

(62) Brito, R. M. M.; Vaz, W. L. C. Determination of the Critical Micelle Concentration of Surfactants Using the Fluorescent Probe N-Phenyl-1 − naphthylamine. *Anal. Biochem.* **1986**, *152*, 250−255.

(63) Roy, S.; Mohanty, A.; Dey, J. Microviscosity of bilayer membranes of some N-acylamino acid surfactants determined by fluorescence probe method. *Chem. Phys. Lett.* **2005**, *414*, 23−27.

(64) Tanford, C. Micelle Shape and Size. *J. Phys. Chem. A* **1972**, *76*, 3020−3023.

(65) Nuraje, N.; Bai, H. Y.; Su, K. Bolaamphiphilic molecules: Assembly and applications. *Prog. Polym. Sci.* **2013**, *38*, 302−343.

(66) Mel'nikov, S. M.; Sergeyev, V. G.; Yoshikawa, K. Discrete coil-globule transition of large DNA induced by cationic surfactant. *J. Am. Chem. Soc.* **1995**, *117*, 2401−2408.

(67) Zhu, D.-M.; Evans, R. K. Molecular mechanism and thermodynamics study of plasmid DNA and cationic surfactants interactions. *Langmuir* **2006**, *22*, 3735−3743.

(68) Matulis, D.; Rouzina, I.; Bloomfield, V. A. Thermodynamics of cationic lipid binding to DNA and DNA condensation: roles of electrostatics and hydrophobicity. *J. Am. Chem. Soc.* **2002**, *124*, 7331−7342.

(69) Dutta, P.; Dey, J.; Shome, A.; Das, P. K. Nanostructure formation in aqueous solution of amphiphilic copolymers of 2-(N,N-dimethylaminoethyl)methacrylate and alkylacrylate: Characterization, antimicrobial activity, DNA binding, and cytotoxicity studies. *Int. J. Pharm.* **2011**, *414*, 298−311.

(70) Zhi, D.; Zhang, S.; Cui, S.; Zhao, Y.; Wang, Y.; Zhao, D. The Headgroup Evolution of Cationic Lipids for Gene Delivery. *Bioconjugate Chem.* **2013**, *24*, 487−519.

(71) Mintzer, M. A.; Simanek, E. E. Nonviral Vectors for Gene Delivery. *Chem. Rev.* **2009**, *109*, 259−302.

(72) Kaper, J. B.; Nataro, J. P.; Mobley, H. L. Pathogenic *Escherichia coli*. *Nat. Rev. Microbiol.* **2004**, *2*, 123−140.

(73) Hennekinne, J. A.; De Buyser, M. L.; Dragacci, S. *Staphylococcus aureus* and its food poisoning toxins: characterization and outbreak investigation. *FEMS Microbiol. Rev.* **2012**, *36*, 815−836.